Promega

Innovative bioluminescence assay technology, customized to your requirements.

Fit-for-purpose reagents make it easy.

Let's TALK CUSTOM

HIGH THROUGHPUT

APPLICATION-SPECIFIC DESIGNS

40+ years CUSTOM EXPERIENCE

Selecting a supplier for your drug discovery and development assays can be a challenge—especially a supplier who can adapt to your specific needs. Don't settle for just a supplier. Instead, partner with Promega and work with a custom manufacturer willing to provide you with the scientific expertise, ongoing technical support and quality standards that support your success.

Watch the video or download a PDF:
promega.com/CustomBioluminescence

Received: 11 January 2018 | Revised: 13 February 2018 | Accepted: 14 February 2018
DOI: 10.1002/bit.26568

ARTICLE

WILEY BIOTECHNOLOGY & BIOENGINEERING

Application of adaptive laboratory evolution to overcome a flux limitation in an *Escherichia coli* production strain

Kento Tokuyama[1] | Yoshihiro Toya[1] | Takaaki Horinouchi[2] | Chikara Furusawa[2,3] | Fumio Matsuda[1,4] | Hiroshi Shimizu[1]

[1] Department of Bioinfomatic Engineering, Graduate School of Information Science and Technology, Osaka University, Suita, Osaka, Japan

[2] Quantitative Biology Center, RIKEN, Suita, Osaka, Japan

[3] Universal Biology Institute, The University of Tokyo, Hongo, Tokyo, Japan

[4] RIKEN Center for Sustainable Resource Science, Tsurumi-ku, Yokohama, Japan

Correspondence
Hiroshi Shimizu, Department of Bioinfomatic Engineering, Graduate School of Information Science and Technology, Osaka University, 1-5 Yamadaoka, Suita, Osaka, 565-0871, Japan.
Email: shimizu@ist.osaka-u.ac.jp

Funding information
Japan Society for the Promotion of Science, Grant numbers: Grant-in-Aid for JSPS Fellows (15J06350), Grant-in Aid for Scientific Research (B)16H04576

Abstract

Gene deletion strategies using flux balance analysis (FBA) have improved the growth-coupled production of various compounds. However, the productivities were often below the expectation because the cells failed to adapt to these genetic perturbations. Here, we demonstrate the productivity of the succinate of the designed gene deletion strain was improved by adaptive laboratory evolution (ALE). Although FBA predicted deletions of *adhE-pykAF-gldA-pflB* lead to produce succinate from glycerol with a yield of 0.45 C-mol/C-mol, the knockout mutant did not produce only 0.08 C-mol/Cmol, experimentally. After the ALE experiments, the highest succinate yield of an evolved strain reached to the expected value. Genome sequencing analysis revealed all evolved strains possessed novel mutations in *ppc* of I829S or R849S. In vitro enzymatic assay and metabolic profiling analysis revealed that these mutations desensitizing an allosteric inhibition by L-aspartate and improved the flux through Ppc, while the activity of Ppc in the unevolved strain was tightly regulated by L-aspartate. These result demonstrated that the evolved strains achieved the improvement of succinate production by expanding the flux space of Ppc, realizing the predicted metabolic state by FBA.

KEYWORDS
adaptive laboratory evolution, *Escherichia coli*, flux balance analysis, phosphoenolpyruvate carboxylase, succinate production

1 | INTRODUCTION

One of the goals of metabolic engineering is to optimize a metabolic system for overproduction of a target compound based on the understanding of the system. Recent developments in genome-scale metabolic reconstructions have enabled the simulation of the physiological characteristics of organisms (Feist & Palsson, 2008; McCloskey, Palsson, & Feist, 2013; Oberhardt, Palsson, & Papin, 2009). Flux balance analysis (FBA) is a method to estimate a metabolic flux distribution using a genome-scale metabolic model (Chen, Alonso, Allen, Reed, & Shachar-Hill, 2011; Kauffman, Prakash, & Edwards, 2003; Orth, Thiele, & Palsson, 2010; Varma & Palsson, 1994), and it has been widely used to predict the effect of gene knockouts in enhancing the target production (Alper, Jin, Moxley, & Stephanopoulos, 2005; Burgard, Pharkya, & Maranas, 2003; Chowdhury, Zomorrodi, & Maranas, 2014; Feist et al., 2010; Fowler, Gikandi, & Koffas, 2009; Ohno, Furusawa, & Shimizu, 2013; Ohno, Shimizu, & Furusawa, 2014; Xu, Ranganathan, Fowler, Maranas, & Koffas, 2011).

Gene knockout mutant for growth-coupled target production can be screened by comparing production yield at its maximum growth state as predicted by FBA (Burgard, Pharkya, & Maranas, 2003; Feist et al., 2010; Ohno, Shimizu, & Furusawa, 2014). The knockout mutant must produce a target metabolite to produce the biomass components with satisfying the mass balance constraints. Several studies

successfully achieved strain improvement for production of various target metabolites by using such simulations (Lee et al., 2005; Ng, Jung, Lee, & Oh, 2012; Tokuyama et al., 2014; Yim et al., 2011). However, these knockout mutants often showed lower cell growth ability and target production yield as compared to FBA predictions (Supplementary Table S1). These inconsistencies should be arise from the flux space of actual metabolic network, which is diminished by kinetic constraints such as enzymatic regulation (Machado, Herrgård, & Rocha, 2015), expression regulation (Covert, Schilling, & Palsson, 2001), and thermodynamic feasibility (Hamilton, Dwivedi, & Reed, 2013), and as a result, the knockout mutant could not achieve the optimal growth state as predicted by FBA.

Adaptive laboratory evolution (ALE) is a useful approach for increasing cell growth rate (Elena & Lenski, 2003; Lenski et al., 1998; Sandberg et al., 2014) and optimizing the metabolic state to FBA predictions (Conrad, Lewis, & Palsson, 2011; Fong et al., 2005; Fong & Palsson, 2004; Ibarra, Edwards, & Palsson, 2002). Previously, Fong and Palson (2004) reported that integrated use of FBA and ALE increased cell growth rates of the *E. coli* knockout mutants to their optimal growth state, and optimized their flux distribution in the metabolic network for target production (Fong et al., 2005). However, the molecular mechanisms behind the changes in the activity of metabolic pathways, cell growth, and target production were unclear in these studies. Moreover, the cause of inconsistencies between the predicted value and the obtained result for the unevolved knockout mutant is still not explained.

In the present study, we designed a knockout mutant of *E. coli* for growth-coupled succinate production. It did not reach to the optimal growth state and decreased the productivity compared with the prediction. High succinate producing strains were obtained by ALE experiment of the knockout mutant. Experimental analyses of genome, enzyme, and metabolome in the strains revealed that a kinetic limitation diminished the flux space of actual metabolic network, and therefore the knockout mutant couldnot reach to the optimal growth state. The present result have also demonstrated that novel mutations occurred during ALE expanded the flux space by reducing the kinetic constraint for growth-coupled succinate production from glycerol in *E. coli*.

2 | MATERIALS AND METHODS

2.1 | Metabolic simulation

The genome-scale metabolic model of *E. coli* K-12, named iAF1260 (Feist et al., 2007), was used for the study. All simulations were performed using MATLAB (MathWorks Inc., Natick, MA) with a solver for linear programming, Gurobi (http://www.gurobi.com).

2.2 | Multiple knockout simulation for growth-coupled succinate production

In order to identify the candidates for gene knockout to achieve production of succinate coupled with cell growth, FBA was performed on comprehensive knockout models of iAF1260 as previously described (Tokuyama et al., 2014). Glycerol was used as the sole carbon source in metabolic simulations, and glycerol uptake rate (GUR) was set to 15 mmol g cell dry weight $(CDW)^{-1}$ hr^{-1}. The oxygen uptake rate (OUR) was set to 10 mmol $gCDW^{-1}$ hr^{-1}. Other external metabolites such as CO_2 and NH_3 were allowed to transport freely through the cell membrane.

2.3 | Flux balance analysis with constraints of measured fluxes

Function of optimize CbModel in COBRA Toolbox (Schellenberger et al., 2011) was used to calculate metabolic flux distributions on continuous cultivation with setting allowLoops to false. In order to avoid undetermined fluxes due to the genome-scale metabolic reconstruction, constraint based metabolic flux analysis was performed using the core *E. coli* metabolic model (http://gcrg.ucsd.edu/Downloads/EcoliCore). For considering glycerol assimilation pathway, the reactions of EX_glyc(e), GLYCtex, GLYK, G3PD5, GLYCDx, DHAPT, and F6PA in the genome-scale metabolic model iAF1260 were added to the core *E. coli* metabolic model and the flux of the reactions corresponding to the knockout genes were set to zero. Experimentally measured GUR, cell growth rate and production rates for succinate, acetate, lactate, ethanol, and formate were used to fix their flux, and then ATP maintenance reaction was maximized as an objective function, because previous studies demonstrated maximization of the ATP maintenance achieved the highest predictive accuracy of metabolic flux distributions under the continuous cultivations (Ow, Lee, Yap, & Oh, 2009; Schuetz, Kuepfer, & Sauer, 2007).

2.4 | Protein structural analysis

The protein structure of Ppc from *E. coli* Kai et al. (1999) (PDB ID: 1FIY) was obtained from the Protein Data Bank (http://www.rcsb.org/pdb/home/home.do). Structure visualization and introduction of identified mutations were carried out using Pymol (http://www.pymol.org).

2.5 | Strains and plasmids

All strains and plasmids used in this study are listed in Supplementary Table S2. BW25113 was used as the succinate production host. BW25113 *ΔadhE ΔpykAF ΔgldA::kan ΔpflB::tet* was constructed by Wanner's method (Datsenko & Wanner, 2000) and P1 phage transduction (Thomason, Costantino, & Court, 2007). *E. coli* strain DH5α was used for plasmid construction and *E. coli* strain BL21(DE3) was used for enzymatic analysis. Phosphoenolpyruvate carboxylase (Ppc) was expressed in pET28-a(+) (Novagen, Madison, WI).

2.6 | Adaptive laboratory evolution

Adaptive laboratory evolution was performed in 5 ml of M9 minimal medium (16.9 g/L $Na_2HPO_4 \bullet 12H_2O$; 3.1 g/L KH_2PO_4; 1.0 g/L NH_4Cl; 0.5 g/L NaCl; 0.493 g/L $MgSO_4 \bullet 7H_2O$; 0.0147 g/L $CaCl_2 \bullet H_2O$)

supplemented with 10 g/L glycerol, 1% (v/v) wolfe's mineral, and 1% (v/v) wolfe's vitamin at 37 °C with shaking at 20 strokes min^{-1} using Bio-Photorecorder TVS062CA (Advantec Toyo Co., Tokyo, Japan). Optical density at 660 nm was automatically monitored every 20 min during the cultivation to determine the maximum specific growth rate. From the stationary phase culture, 1 µl of broth was passaged into fresh medium. In 100.1 ± 0.3 generations, evolved strains, named strain A-E, were isolated from the culture broth of five parallel passaged cultivations.

2.7 | Batch culture protocol

The evolved *E. coli* strains (strain A-E) and parent strain (strain P, BW25113 *ΔadhE ΔpykAF ΔgldA::kan ΔpflB::tet*), wildt-ype *E. coli* (strain W, BW25113) were inoculated from the glycerol stock to 5 ml M9 medium and cultured aerobically at 37 °C overnight. The overnight cultures were transferred to fresh 50 ml M9 medium maintaining an initial optical density of 0.05 at 600 nm (OD_{600}). Cells were cultured in a 100 ml Erlenmeyer flask at 37 °C and incubated in a rotary shaking incubator at 150 rpm (BR-43FL, Taitec, Saitama, Japan).

2.8 | Continuous culture protocol

Strain B and P were inoculated from the glycerol stock to 40 ml M9 medium and aerobically cultured at 37 °C overnight. The culture broths were transferred to fresh 600 ml M9 medium in a 1-L jar fermenter, BMJ-P type bioreactor (ABLE, Tokyo, Japan) equipped with temperature, pH, and dissolved oxygen sensor. The temperature was maintained at 37 °C and pH was set at 7.0 using NH_3 solution. Air flow rate and agitation speed were set at 300 ml/min and 400 rpm, respectively. The inoculum size was set to an initial OD_{600} of 0.1. After 8 hr of cultivation in batch mode, the continuous culture mode was started with a dilution rate of 0.04 hr^{-1}. After 48 hr into the continuous mode, the agitation speed was reduced to 100 rpm, and the culture broth were collected after more than two residence times for quantitation of extracellular metabolites.

2.9 | Analytical methods

Cell growth was monitored by the measurement of OD_{600} using UV-mini 1240 (Shimadzu, Kyoto, Japan). Concentrations of glycerol, succinate, lactate, acetate, formate, and ethanol present in the culture supernatant were determined by high performance liquid chromatography (HPLC Prominence, Shimadzu) equipped with an Aminex HPX-87H column (Bio-Rad, Hercules, CA), a UV/vis detector (SPD-20A), and a refractive index detector (RID-10A) under the measurement conditions previously described (Tokuyama et al., 2014).

2.10 | Genome sequence analysis and mutation analysis

For genomic DNA preparation, the evolved *E. coli* strains (A-E) and parent strain P, wild-type *E. coli* were inoculated from the glycerol stock to 5 ml M9 medium and aerobically cultured at 37 °C overnight. Subsequently, rifampicin (300 µg/ml final concentration) was added and the culture was continued for further 3 hr to block the initiation of DNA replication. The cells were collected by centrifugation at 20,000*g* for 1 min, at 4 °C, and the pelleted cells were stored at −80 °C until genomic DNA preparation. The genomic DNA was extracted from cell pellets of strain P and evolved strains A-E by DNeasy Blood & Tissue Kit (Qiagen, Germany) in accordance with the manufacturer's instructions. Genome sequence analysis were performed with MiSeq Desktop Sequencer (Illumina, Inc., San Diego, CA) as described previously (Horinouchi, Sakai, Kotani, Tanabe, & Furusawa, 2017). The reads obtained were aligned to the reference sequence of *E. coli* BW25113 genomic DNA (GenBank: NZ_CP009273) using breseq pipeline, version 0.28 (Deatherage & Barrick, 2014). The mutations of *ppc* identified in all evolved strains were confirmed by Sanger sequence analysis of PCR products by Value Read sequencing service (Eurofins Genomics, Tokyo, Japan). Genome sequence data of *E. coli* strains in this study were deposited in the DDBJ Sequence Read Archive of the DNA Data Bank of Japan (DRA) under accession number DRA006046.

2.11 | Reverse engineering of identified *ppcppc* mutations

Mutations identified in *ppc* were introduced into the genome of strain P by multiplexed automated genome engineering (MAGE) using pORTMAGE-2 vector (Nyerges et al., 2016). pORTMAGE-2 was a gift from Csaba Pál (Addgene plasmid #72677). Sequences of MAGE oligos were created by MODEST tool (Bonde et al., 2014) as shown in Supplementary Table S3 and the oligos were synthesized by FASMAC Co., Ltd. (Kanagawa, Japan). We have inserted the mutations of *ppc* in strain P to make its genotype the same as that of the evolved strain B or C following the procedure reported previously (Nyerges et al., 2016).

2.12 | Molecular cloning and enzyme overexpression

The *ppc* genes were amplified by PCR using KOD FX Neo (Toyobo Co., Ltd., Osaka, Japan) from the genomic DNA of strain P, B, and C using the primers as shown in Supplementary Table S4. Each amplified fragment was treated with A-attachment mix (Toyobo Co., Ltd.), and then cloned into pGEM-T Easy (Promega Co., Madison, WI), followed by sequence confirmation by Value Read sequencing service (Eurofins). The *Nde*I-*Xho*I fragments of pGEM-T Easy were cloned into the same restriction site of pET28-a(+) vector, generating pET28-a(+)/ppc^{wild}, pET28-a(+)/ppc^{I829S}, and pET28-a(+)/ppc^{R849S}. The recombinant strains of BL21(DE3) harboring the plasmids were cultured in LB medium at 37 °C overnight. Five hundred micro liters of the culture broths were transferred to 250 ml baffled Erlenmeyer flasks containing fresh 50 ml LB medium containing 0.1 mM isopropyl-β-d-thiogalactopyranoside and cultured at 30 °C in a rotary shaking incubator at 200 rpm (BR-43FL, Taitec). After 20 hr of cultivation, the cells pellets were obtained from 10 ml of culture broth by centrifugation at 2,500*g* for 5 min at 4 °C.

2.13 | Enzymatic assay of wild-type ppc and its mutant with L-aspartate

The enzyme activity of the purified Ppc was assayed by a coupling reaction catalyzed by malate dehydrogenase at 30 °C as previously described (Chen, Bommareddy, Frank, Rappert, & Zeng, 2014). The standard reaction mixture contained 100 mM Tris-HCl (pH 7.5), 10 mM $MnSO_4$, 10 mM $NaHCO_3$, 2 mM PEP, 0.1 mM NADH, and 1.5 U of malate dehydrogenase (Sigma–Aldrich Co, St. Louis, MI). The decrease in absorbance of NADH at 340 nm was monitored by a microtiter plate reader (Varioskan Flash Multimode Reader, Thermo Fisher Scientific, Waltham, MA).

2.14 | Metabolome analysis

Twenty milliliters of culture broth from the batch culture experiment was sampled rapidly during the exponential growth phase and filtered through a 0.5 μm pore size filter (PTFE-type membrane, Advantec, Tokyo, Japan). Cells on the filter were immediately immersed in 1.6 ml methanol (−80°C) containing 5 μM cycloleucine as an internal standard for the quantitation with GC-MS. Following addition of 1.6 ml of chloroform (−30°C) and 640 μl of Milli-Q water (4°C) and vortexing for 1 min, the mixture was centrifuged at 3,700*g* for 20 min at 4 °C. The aqueous layer was dispensed into seven Eppendorf tubes by 300 μl and dried using a SpeedVac SPD1010 (Thermo Fisher Scientific, Waltham, MA) at room temperature.

Gas chromatography–mass spectrometry (GCMS-QP2010 Ultra, Shimadzu, Japan) was performed under the following conditions. The column used was DB-5MS + DG column (30 m × 0.25 mm ID × 0.25 μm, Agilent Technologies, Santa Clara). The front inlet temperature was set to 250 °C. The helium gas flow rate through the column was at 1 ml/min. The column temperature was held at 70 °C for 2 min isothermally and later raised by 3 °C/min to 280 °C and held there for 3 min isothermally. The transfer line and ion-source temperatures were 250 °C and 200 °C, respectively. The dried extract was dissolved in 25 μl methoxyamine hydrochloride (20 mg/ml-pyridine) and incubated at 37 °C for 90 min. For *tert*-butyldimethylsilylation, 25 μl of *N*-(*tert*-butyldimethylsilyl)-*N*-methyltrifluoroacetamide containing 1% *tert*-butyldimethylchlorosilane was added and incubated at 60 °C for 30 min. After 2 hr cooling, the samples were centrifuged at 21,500*g* for 5 min. One micro liters of the supernatant containing the derivatized samples were injected at a split injection ratio of 1:10.

Intracellular concentration of each metabolite (mmol/L-cell) was determined based on their peak area of the MS data, collected cell volumes, and the aqueous cell volume and dry weight of one *E. coli* (4.96×10^{-16} L/cell and 2.8×10^{-13} g CDW/cell, respectively) (Neidhardt, 1996).

3 | RESULTS AND DISCUSSION

3.1 | In silico strain design and its experimental evaluation

Genome scale metabolic model iAF1260 (Feist et al., 2007) was used to identify gene deletion candidates for succinate production from glycerol coupled with cell growth. Since ethanol is a major byproduct of *E. coli* fermentation on glycerol medium, combinatorial knockouts of triple reaction were simulated on the iAF1260 disrupting the reactions encoded by *adhE*. Combinatorial deletion mutant of *adhE-pykAF-gldA-pflB* was predicted as the highest succinate producer, and was expected to produce 0.45 C-mol/C-mol of succinate at the maximal cell growth. FBA simulations predicted that wild-type *E. coli* catabolized glycerol via glycolysis, and formed acetate, ethanol, and formate (Figure 1a), whereas the knockout mutant produced succinate via phosphoenolpyruvate carboxylase (Ppc) and reductive TCA cycle (Figure 1b).

Based on the FBA prediction, candidate genes (*adhE-pykAF-gldA-pflB*) were disrupted in wild-type *E. coli* BW25113, generating parent strain (strain P). The strain was cultivated in M9 medium using Erlenmeyer flasks. Although succinate yield from strain P (0.08 ± 0.00 C-mol/C-mol) was improved threefold in comparison with the wild-type strain (0.03 ± 0.00 C-mol/C-mol) (Figure 2a and Table 1), the productivity was lower than of the predicted value by FBA (0.45 C-mol/C-mol).

3.2 | Improvement of productivity by adaptive laboratory evolution

Since the metabolic pathway of strain P was designed for growth-coupled succinate production, the evolved mutants with improved growth via ALE would have enhanced succinate production. Five evolved strains (strain A–E) were obtained by parallel passage of cultivations for 100.1 ± 0.3 generations (Supplementary Figure S1). The specific growth rates were improved by more than twofold during ALE experiments. All of the evolved strains successfully increased the yield of succinate by more than 3.1-fold in flask cultivation (Figure 2a). Strain B and C were the highest producers of succinate with 0.33 ± 0.03 and 0.33 ± 0.04 C-mol/C-mol yields, respectively. During the continuous cultivation, strain P showed almost no production of succinate, on the other hand strain B showed the higher yields of succinate with 0.45 C-mol/C-mol yield, as predicted by FBA simulation (Figure 2b). The biomass yield in strain B was almost the same as the predicted value. Furthermore, byproduct formations such as acetate and lactate were consistent with the FBA result (Table 1).

3.3 | Mutation analysis and elucidation of molecular mechanism of productivity improvement

For elucidating the molecular mechanism of the decreased succinate production in the unevolved knockout mutant, genomes of all evolved strains and strain P were sequenced using high-throughput sequencer Illumina MiSeq. The raw sequences generated, $5.3–6.5 \times 10^8$ base pairs, showed an average coverage of approximately 100-140-fold of 4.63×10^6 *E. coli* BW25113 genome (GenBank: NZ_CP009273). Mutations were identified by the breseq pipeline (Deatherage & Barrick, 2014) using the genome sequence of *E. coli* BW25113 as reference. All of the evolved strains had more than one mutation in coding regions of *ytfT*, *cyaA*, *glpK*, *ppc*, and *eutH* (Table 2). Especially, mutations of *ppc* encoding

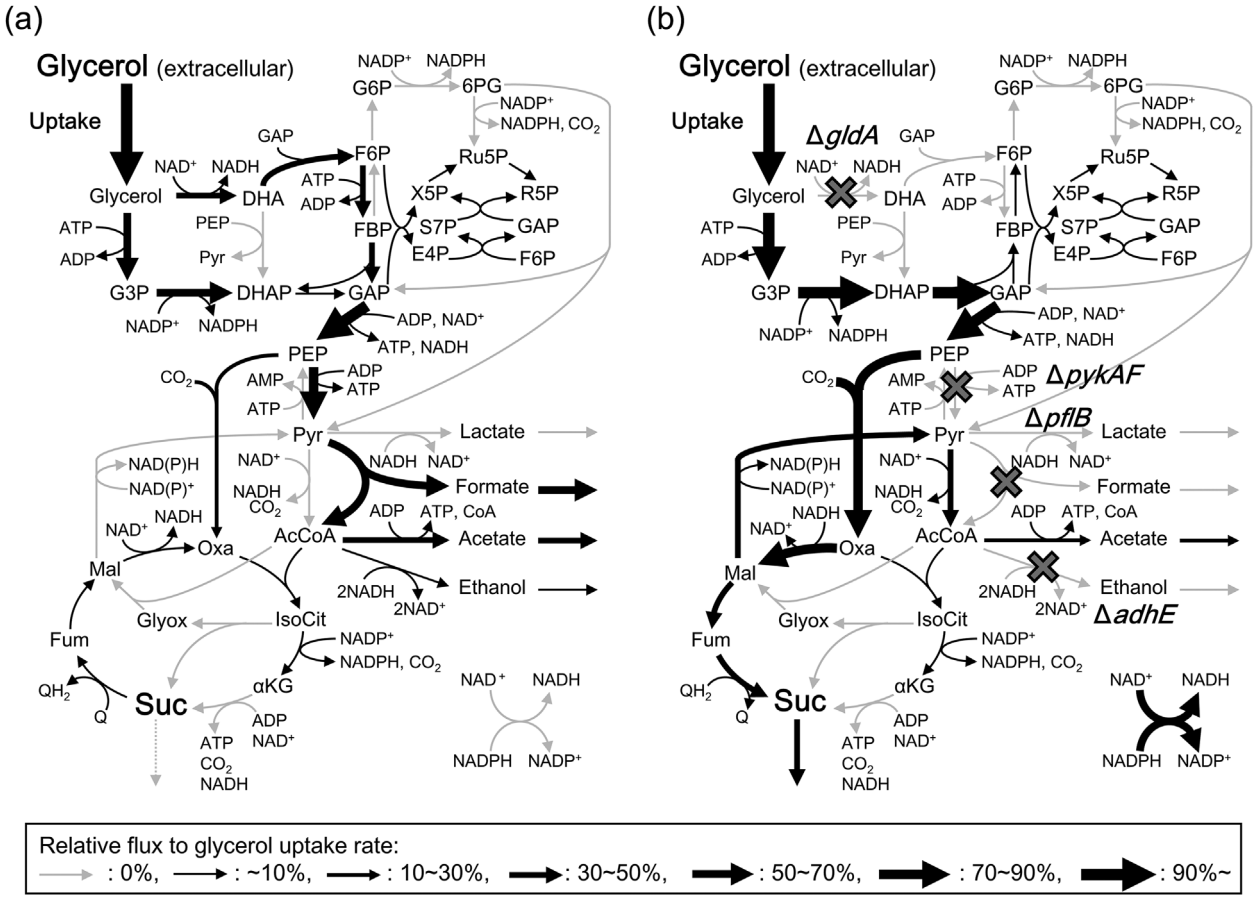

FIGURE 1 Metabolic simulation for growth-coupled succinate production. Flux distributions of wild-type *E. coli* (a) and knockout mutant of *adhE-pykAF-gldA-pflB* (b) at optimal growth state were calculated by using genome-scale metabolic model iAF1260

Ppc were shared at I829S in strain A and B or R849S in strain C, D, and E, and strain B, C, D had a only the mutation in *ppc*. These results suggested that the reaction of Ppc had kinetic limitations for achieving the optimal metabolic state, and introduction of these mutations in *ppc* led to changes in the enzyme properties for enhancing the activity.

To evaluate the effect of these identified mutations on succinate production, mutations in *ppc* were introduced into the genome of strain P by multiplexed genome engineering. Introducing mutations of I829S or R849S in strain P improved the cell growth rate by about 2.0-fold, and increased the yield of succinate to 0.29 ± 0.01 or 0.28 ± 0.02

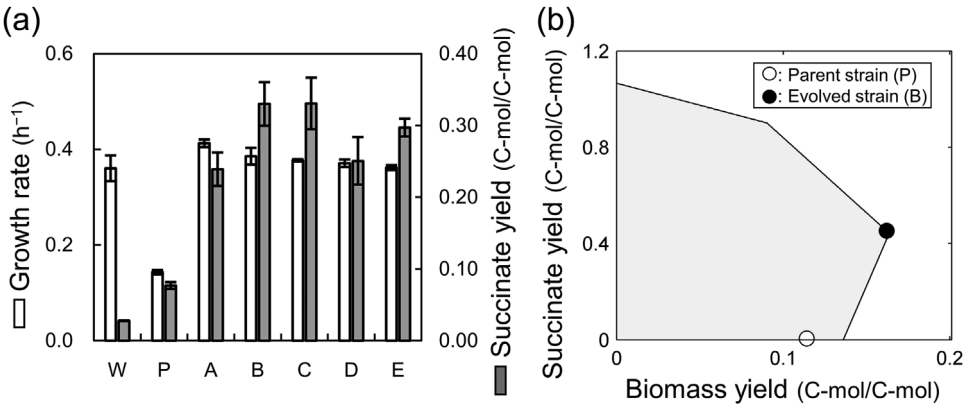

FIGURE 2 Culture result of adaptive laboratory evolution. (a) Specific growth rate and succinate production in a batch culture. The cells obtained after 100 generations on M9 medium were named as "strain A" - "strain E" in the descending order of growth rate. W and P indicate wild-type *E. coli* BW25113 and the knockout strain of *adhE-pykAF-gldA-pflB*, respectively. (b) Direct comparison of feasible solution space and experimental results of continuous culture. White and black circles indicate the experimental results of strain P and B. Metabolic solution space was calculated with measured values of GUR and OUR in the knockout model of iAF1260 (gray area). For the calculation, GUR, and OUR were set to the experimentally measured values of 3.37 mmol $gCDW^{-1}$ hr^{-1} and 2.85 mmol $gCDW^{-1}$ hr^{-1} in strain B, respectively

TABLE 1 Summary of the carbon-molar yield.

Condition & strains	Biomass[a] (C-mol/C-mol)	Succinate (C-mol/C-mol)	Lactate (C-mol/C-mol)	Acetate (C-mol/C-mol)	Ethanol (C-mol/C-mol)
Batch culture					
(W): Wild-type	0.20 ± 0.01	0.03 ± 0.00	0.11 ± 0.00	0.19 ± 0.01	0.24 ± 0.02
(P): Parent	0.35 ± 0.01	0.08 ± 0.00	0.18 ± 0.15	0.12 ± 0.01	0
(A): Evolved A	0.44 ± 0.04	0.24 ± 0.02	0	0.23 ± 0.02	0
(B): Evolved B	0.27 ± 0.02	0.33 ± 0.03	0.08 ± 0.01	0.26 ± 0.02	0
(C): Evolved C	0.31 ± 0.04	0.33 ± 0.04	0.06 ± 0.01	0.28 ± 0.03	0
(D): Evolved D	0.25 ± 0.04	0.25 ± 0.03	0.05 ± 0.01	0.22 ± 0.03	0
(E): Evolved E	0.28 ± 0.01	0.30 ± 0.01	0.06 ± 0.01	0.26 ± 0.01	0
I829S mutant[b]	0.28 ± 0.03	0.29 ± 0.01	0.02 ± 0.00	0.26 ± 0.02	0
R849S mutant[b]	0.26 ± 0.02	0.28 ± 0.02	0.01 ± 0.00	0.27 ± 0.02	
I829S-R849S mutant[b]	0.24 ± 0.01	0.28 ± 0.01	0.03 ± 0.00	0.25 ± 0.01	
Continuous culture			0		0
(P): Parent	0.11	0.01	0	0.14	0
(B): Evolved B	0.16	0.45	0	0.29	0
Simulation[c]					
(P): Parent	0.29	0.32	0	0.29	0
(B): Evolved B	0.16	0.44	0	0.32	0

[a]For calculation of biomass yield, OD_{600} was converted into dry cell weight using the conversion coefficient of 0.3 gCDW • L^{-1} • $OD_{600}{}^{-1}$, and carbon-mol in the biomass was calculated based on the biomass composition described in the iAF1260 model.
[b]These strains were constructed by introducing of the identified *ppc* mutations into the genome of strain P.
[c]The values were calculated by FBA using the genome-scale metabolic model iAF1260 adding constraints of experimentally measured values for GUR at 4.77 and 3.37 mmol $gCDW^{-1}$ hr^{-1}, and OUR at 4.14 and 2.85 mmol $gCDW^{-1}$ hr^{-1} in strain P and B, respectively.

C-mol/C-mol, respectively, which were 89% or 84% of the yield from the highest producers, strain B and C (Table 1 and Supplementary Figure S2). These results indicated that the mutations identified in *ppc* were important for succinate production in strain P. On the other hand, the engineered mutant containing both the I829S and R849S mutations displayed the same amount of succinate production as the single mutants (Supplementary Figure S2). Since there was no synergistic effect of the two mutations on succinate production, these mutations likely affect the same enzymatic characteristics.

The slight differences between the engineered strains constructed from strain P and the evolved strains obtained from ALE might be caused by potential genomic duplications and deletions mediated by IS family. The mutation analysis using breseq ver 0.28 revealed that some regions were unassigned new junction evidence to the reference genome of *E. coli* BW25113, and a potential insertion in the *uspC-flhDC* intergenic region (*flhD/uspC*, −513/−267) mediated by IS5 were shared in all evolved strains. This insertion might improve the resistance of evolved strains for environmental stress and increase the growth coupled succinate production in the evolved strains (Zhi, Banting, Ruecker, & Neumann, 2017).

3.4 | Functional analysis of the mutations of Ppc

For characterization of the mutated amino acid residues of Ppc, multiple sequence alignment was performed with clustalW (Kyoto University Bioinformatics Center: http://clustalw.genome.jp, Supplementary Figure S3). The isoleucine residue at position 829 in *E. coli* Ppc is conserved in *Mannheimia succinicproducens* and *Thermus thermophilus* HB8, whereas other microorganisms including *Corynebacterium glutamicum* have a valine residue at the equivalent position of Ile829 in *E. coli*. The arginine residue at position 849 is highly conserved in various microorganisms. Functional analysis of the mutants of Ppc was performed to understand how the identified mutations in *ppc* changed enzymatic properties. Protein structure of Ppc has been reported previously by Kai et al. (1999). The model displayed that the mutated positions at Ile829 and Arg849 residues were in the same α-helix strand (Figure 3a, yellow). Four residues, Lys773, Arg832, Arg587, and Asn881, are involved in L-aspartate binding, and among these, Arg832 is located in the same α-helix strand that contains Ile829 and Arg849 (Figure 3b). Because L-aspartate allosterically inhibits Ppc, it was hypothesized that the I829S and R849S mutations should decrease the inhibition by aspartate, leading to an increase in the flux of Ppc for succinate synthesis. Protein structure model of I829S mutant of Ppc suggests that the mutation pushes the residue of Arg832 away from L-aspartate binding by forming a hydrogen bond (2.9 Å) between the hydroxyl residue of Ser829 and the amino group of Arg832 (Figures 3b and 3c). Arg849 residue has a hydrogen bond with the residue of Leu63 (Figure 3d). Because the mutated residue of Ser849 cannot bind the residue of Leu63, the R849S mutant should change the tertiary structure of Ppc, and decrease the affinity for L-aspartate (Figure 3e).

TABLE 2 Identified mutations in the evolved strains

Strain	Gene	Mutation	Type	Enzyme
A	*ytfT*	C393T	I130I (Synonymous)	Sugar ABC transporter permease
	cyaA	+C (1901/2547t)	Frameshift	Adenylate cyclase
	glpK	G762T	Q254H	Glycerol kinase
	ppc	T2486G	I829S	Phosphoenolpyruvate carboxylase
B	*ppc*	T2486G	I829S	Phosphoenolpyruvate carboxylase
C	*ppc*	C2545A	R849S	Phosphoenolpyruvate carboxylase
D	*ppc*	C2545A	R849S	Phosphoenolpyruvate carboxylase
E	*ppc*	C2545A	R849S	Phosphoenolpyruvate carboxylase
	eutH	C936A	N312K	Ethanolamine transporter

The effect of the replacement of Ile829 or Arg849 by serine in Ppc was examined by in vitro enzymatic analysis. The enzymatic activities of Ppc in crude lysates were measured by a coupling reaction catalyzed by malate dehydrogenase and measuring the absorbance of NADH at 340 nm. The activity of wild-type Ppc (Ppc^{Wild}) was drastically decreased by ca. 78% in the presence of 1 mM L-aspartate with 4 mM PEP (Figure 3f). On the other hand, Ppc mutants (Ppc^{I829S} and Ppc^{R849S}) displayed lower levels of the inhibition compared to Ppc^{wild} (Figures 3g and 3h). Especially, Ppc^{I829S} showed no sensitivity to L-aspartate inhibition with different concentrations of PEP tested from 0.2 mM to 4 mM.

3.5 | Metabolic profiling analysis

For verification of in vivo effect of allosteric inhibition of L-aspartate to Ppc, intracellular metabolites in central carbon metabolism and amino

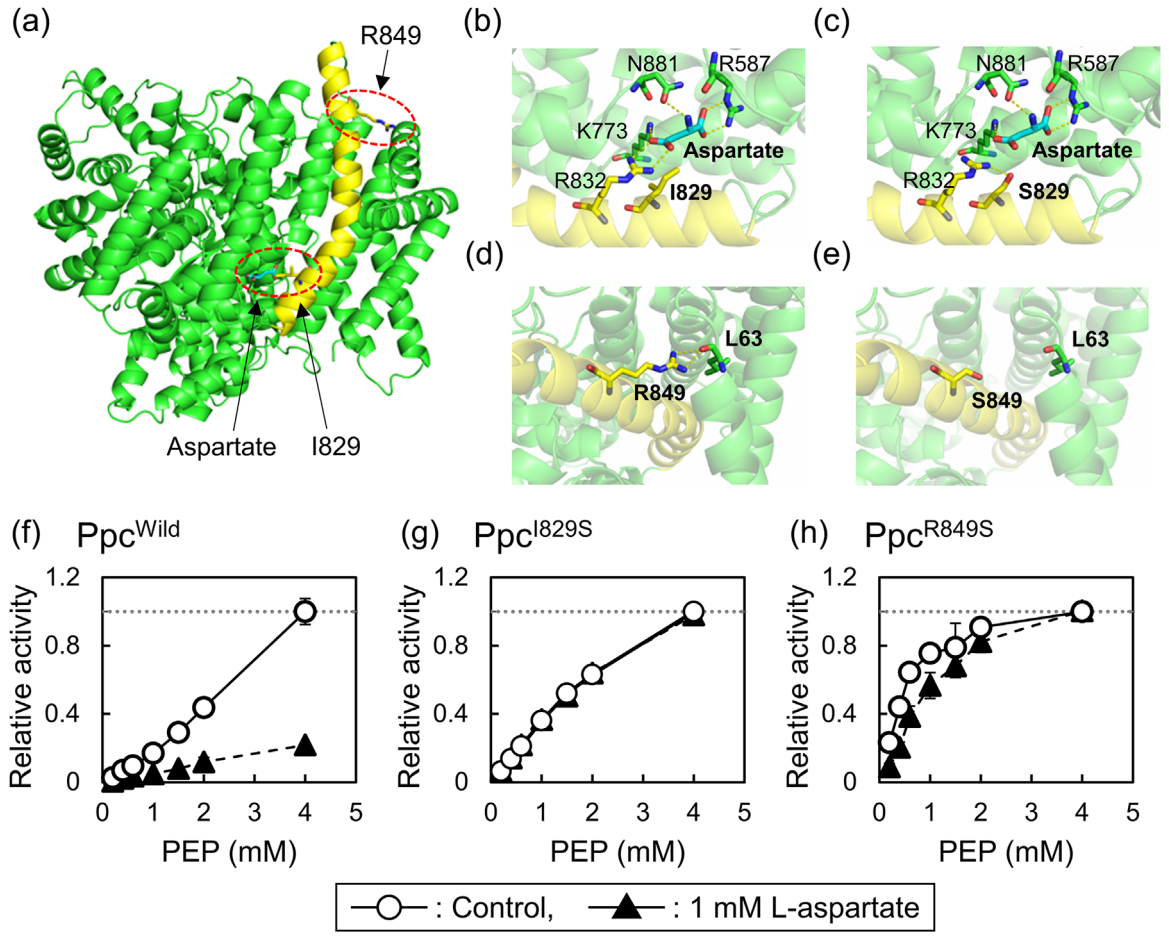

FIGURE 3 Functional analysis of identified mutations in Ppc. (a) Protein structure of Ppc wild-type monomer. (b–e) Close view of mutated site for I829S (b and c), and R849S (d and e). Yellow dashed line indicated hydrogen bonds (<3.2 Å). (f–h) Specific activity of Ppc of wild-type (f), I829S mutant, (g) and R849S mutant (h) with (black triangle) or without (open circle) 1 mM aspartate. The values indicate the relative activities against the activity with 4 mM PEP and in the absence of L-aspartate

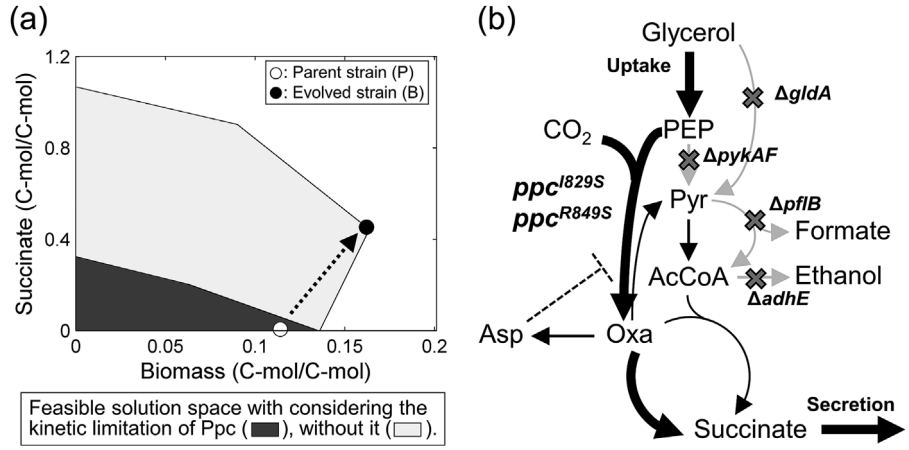

FIGURE 4 Adaptation trajectory of the knockout mutant for improving succinate production. (a) Computationally predicted feasible solution space in metabolic network with or without considering the kinetic limitation of Ppc. Experimentally measured GUR and OUR of strain B were considered as constraints, and the upper bounds of Ppc flux was set to free or 2.8% of GUR. White and black circles indicate the experimental results of strain P and B. (b) Overview of metabolic evolution for succinate production demonstrated in this study

acids were quantified by gas chromatography–mass spectrometry (Supplementary Figure S4). Aspartate concentration in strain P was 3.05 ± 0.35 mM, which was three times higher than the concentration that could cause 78% inactivation of Ppc activity in vitro. Furthermore, PEP in strain P was 12.5-fold higher than of wild-type *E. coli* (6.04 ± 0.20 mM and 0.48 ± 0.06 mM, respectively). Compared with the accumulations of these metabolites in strain P, aspartate concentration in strain B had no significant change (2.72 ± 0.35 mM), on the other hand, PEP concentrations was drastically decreased to 0.75 ± 0.10 mM. These results indicated that the evolved strains could overcome this metabolic limitation by introducing single amino acids substitution of Ile829Ser or Arg849Ser in Ppc.

Flux distribution calculated by FBA with constraints of measured fluxes indicated that Ppc flux of strain P on continuous cultivation was 2.8% of GUR, whereas strain B showed higher Ppc flux value at 94.5% of GUR (Supplementary Figure S5). Higher accumulation of PEP in strain P (6.04 ± 0.20 mM) than in strain B (0.75 ± 0.10 mM) was also consistent with these results (Supplementary Figure S4). By setting the flux of Ppc to 2.8% of GUR, the knockout mutant model cannot achieve the optimal growth state without any constraints of Ppc (Figure 4a). Therefore, evolved strains alleviate the kinetic limitation of Ppc by introducing single amino acid substitutions generating Ppc^{I829S} or Ppc^{R849S}, and optimized their metabolic network to improve succinate production as expected by FBA (Figure 4b).

Ppc^{I829S} and Ppc^{R849S} is thought to be beneficial mutants to development of the other microbial process of valuable chemical production. Ppc is a bottleneck reaction for production of oxaloacetate derived metabolites such as lysine (Contador, Rizk, Asenjo, & Liao, 2009) and 1,4-butanediol (Andreozzi et al., 2016). In other microorganisms such as *C. glutamicum*, Ppc is also thought to be rate limiting reaction since the enzyme is tightly regulated by L-aspartate (Chen et al., 2014; Nakamura, Minoguchi, & Izui, 1996; Takeya, Hirai, & Osanai, 2017). Multiple sequence alignment displayed that the amino acid residues of Ile829 and Arg849 are highly conserved in these microorganisms (Supplementary Figure S3). This indicated that the introduction of mutations identified in Ppc should improve the flux and target production in other microorganisms also.

4 | CONCLUSION

Although there are many reports that the enhanced production of target metabolites using pathway engineering by gene deletion based on in silico design with FBA, most of these applications did not achieve the predicted value at the optimal growth state. One possible cause of these inconsistencies should be certain kinetic constraints, which hampered to optimize metabolic network towards the optimal growth state. In the present study, we firstly designed *E. coli* knockout mutant for growth-coupled succinate production by FBA. It couldnot reach to the predicted optimal growth state. ALE successfully overcame the limitation by introducing novel mutations in *ppc*, and led to improve the succinate production as predicted by FBA. Genome resequencing and functional analysis elucidates the molecular mechanism of rate limiting step of succinate production and the reason why productivity of evolved strain was much improved than that of the parent strain.

ACKNOWLEDGMENTS

This research was supported by a Grant-in-Aid for JSPS Fellows (15J06350), Grant-in Aid for Scientific Research (B)16H04576, and "Program for Leading Graduate Schools" of the Ministry of Education, Culture, Sports, Science and Technology, Japan. We thank Mrs. Hazuki Kotani (QBiC RIKEN, Japan) for help with genome re-sequencing analysis, Dr Csaba Pál (Biological Research Centre of the Hungarian Academy of Sciences, Hungary) for providing pORTMAGE-2 vector, Prof. Kenji Nakahigashi (Keio University, Japan) for providing pKD13Cm and pKD13tet, and Dr Kazufumi Hosoda (Osaka university, Japan) for technical assistance in the enzymatic assay experiment.

ORCID

Hiroshi Shimizu http://orcid.org/0000-0002-8986-0861

REFERENCES

Alper, H., Jin, Y.-S., Moxley, J. F., & Stephanopoulos, G. (2005). Identifying gene targets for the metabolic engineering of lycopene biosynthesis in *Escherichia coli*. *Metabolic Engineering*, *7*, 155–164.

Andreozzi, S., Chakrabarti, A., Soh, K. C., Burgard, A., Yang, T. H., Van Dien, S., … Hatzimanikatis, V. (2016). Identification of metabolic engineering targets for the enhancement of 1,4-butanediol production in recombinant *E. coli* using large-scale kinetic models. *Metabolic Engineering*, *35*, 148–159.

Bonde, M. T., Klausen, M. S., Anderson, M. V., Wallin, A. I. N., Wang, H. H., & Sommer, M. O. A. (2014). MODEST: A web-based design tool for oligonucleotide-mediated genome engineering and recombineering. *Nucleic Acids Research*, *42*, W408–W415.

Burgard, A. P., Pharkya, P., & Maranas, C. D. (2003). Optknock: A bilevel programming framework for identifying gene knockout strategies for microbial strain optimization. *Biotechnology and Bioengineering*, *84*, 647–657.

Chen, X., Alonso, A. P., Allen, D. K., Reed, J. L., & Shachar-Hill, Y. (2011). Synergy between 13C-metabolic flux analysis and flux balance analysis for understanding metabolic adaption to anaerobiosis in *E. coli*. *Metabolic Engineering*, *13*, 38–48.

Chen, Z., Bommareddy, R. R., Frank, D., Rappert, S., & Zeng, A. P. (2014). Deregulation of feedback inhibition of phosphoenolpyruvate carboxylase for improved lysine production in Corynebacterium glutamicum. *Applied and Environmental Microbiology*, *80*, 1388–1393.

Chowdhury, A., Zomorrodi, A. R., & Maranas, C. D. (2014). K-OptForce: Integrating kinetics with flux balance analysis for strain design. *PLoS Computational Biology*, *10*, e1003487.

Conrad, T. M., Lewis, N. E., & Palsson, B. (2011). Microbial laboratory evolution in the era of genome-scale science. *Molecular Systems Biology*, *7*, 509.

Contador, C. A., Rizk, M. L., Asenjo, J. A., & Liao, J. C. (2009). Ensemble modeling for strain development of l-lysine-producing *Escherichia coli*. *Metabolic Engineering*, *11*, 221–233.

Covert, M. W., Schilling, C. H., & Palsson, B. (2001). Regulation of gene expression in flux balance models of metabolism. *Journal of Theoretical Biology*, *213*, 73–88.

Datsenko, K. A., & Wanner, B. L. (2000). One-step inactivation of chromosomal genes in *Escherichia coli* K-12 using PCR products. *Proceedings of the National Academy of Sciences of the United States of America*, *97*, 6640–6645.

Deatherage, D. E., & Barrick, J. E. (2014). Identification of mutations in laboratory-evolved microbes from next-generation sequencing data using bres eq. *Methods in Molecular Biology*, *1151*, 165–188.

Elena, S. F., & Lenski, R. E. (2003). Evolution experiments with microorganisms: The dynamics and genetic bases of adaptation. *Nature Review Genetics*, *4*, 457–469.

Feist, A. M., Henry, C. S., Reed, J. L., Krummenacker, M., Joyce, A. R., Karp, P. D., … Palsson, B. (2007). A genome-scale metabolic reconstruction for *Escherichia coli* K-12 MG1655 that accounts for 1260 ORFs and thermodynamic information. *Molecular Systems Biology*, *3*, 121.

Feist, A. M., & Palsson, B. Ø. (2008). The growing scope of applications of genome-scale metabolic reconstructions using *Escherichia coli*. *Nature Biotechnology*, *26*, 659–667.

Feist, A. M., Zielinski, D. C., Orth, J. D., Schellenberger, J., Herrgard, M. J., & Palsson B. Ø. (2010). Model-driven evaluation of the production potential for growth-coupled products of *Escherichia coli*. *Metabolic Engineering*, *12*(3), 173–186.

Fong, S. S., Burgard, A. P., Herring, C. D., Knight, E. M., Blattner, F. R., Maranas, C. D., & Palsson, B. Ø. (2005). In silico design and adaptive evolution of *Escherichia coli* for production of lactic acid. *Biotechnology and Bioengineering*, *91*, 643–648.

Fong, S. S., & Palsson, B. Ø. (2004). Metabolic gene-deletion strains of *Escherichia coli* evolve to computationally predicted growth phenotypes. *Nature Genetics*, *36*, 1056–1058.

Fowler, Z. L., Gikandi, W. W., & Koffas, M. A. G. (2009). Increased malonyl coenzyme A biosynthesis by tuning the *Escherichia coli* metabolic network and its application to flavanone production. *Applied and Environmental Microbiology*, *75*, 5831–5839.

Hamilton, J. J., Dwivedi, V., & Reed, J. L. (2013). Quantitative assessment of thermodynamic constraints on the solution space of genome-scale metabolic models. *Biophysical Journal*, *105*, 512–522.

Horinouchi, T., Sakai, A., Kotani, H., Tanabe, K., & Furusawa, C. (2017). Improvement of isopropanol tolerance of *Escherichia coli* using adaptive laboratory evolution and omics technologies. *Journal of Biotechnology*, *255*, 47–56.

Ibarra, R. U., Edwards, J. S., & Palsson, B. (2002). *Escherichia coli* K-12 undergoes adaptive evolution to achieve in silico predicted optimal growth. *Nature*, *420*, 186–189.

Kai, Y., Matsumura, H., Inoue, T., Terada, K., Nagara, Y., Yoshinaga, T., … Izui, K. (1999). Three-dimensional structure of phosphoenolpyruvate carboxylase: A proposed mechanism for allosteric inhibition. *Proceedings of the National Academy of Sciences of the United States of America*, *96*, 823–828.

Kauffman, K. J., Prakash, P., & Edwards, J. S. (2003). Advances in flux balance analysis. *Current Opinion in Biotechnology*, *14*, 491–496.

Lee, S. J., Lee, D.-Y., Kim, T. Y., Kim, B. H., Lee, J., & Lee, S. Y. (2005). Metabolic engineering of *Escherichia coli* for enhanced production of succinic acid, based on genome comparison and in silico gene knockout simulation. *Applied and Environmental Microbiology*, *71*, 7880–7887.

Lenski, R. E., Mongold, J. A., Sniegowski, P. D., Travisano, M., Vasi, F., Gerrish, P. J., & Schmidt, T. M. (1998). Evolution of competitive fitness in experimental populations of *E. coli*: What makes one genotype a better competitor than another? *Antonie Van Leeuwenhoek*, *73*, 35–47.

Machado, D., Herrgård, M. J., & Rocha, I. (2015). Modeling the contribution of allosteric regulation for flux control in the central carbon metabolism of *E. coli*. *Frontiers in Bioengineering and Biotechnology*, *3*, 154.

McCloskey D., Palsson B. Ø., & Feist A. M. (2013). Basic and applied uses of genome-scale metabolic network reconstructions of *Escherichia coli*. *Molecular Systems Biology*, *9*, 661.

Nakamura, T., Minoguchi, S., & Izui, K. (1996). Purification and characterization of recombinant phosphoenolpyruvate carboxylase of Thermus sp. *Journal of Biochemistry*, *120*, 518–524.

Neidhardt, F. C., Curtiss, R. (1996). *Escherichia coli and Salmonella*. (2nd ed.). Washington, DC: Amer. Society for Microbiology.

Ng, C. Y., Jung, M., Lee, J., & Oh, M.-K. (2012). Production of 2,3-butanediol in Saccharomyces cerevisiae by in silico aided metabolic engineering. *Microbial Cell Factories*, *11*, 68.

Nyerges, Á., Csörgő, B., Nagy, I., Bálint, B., Bihari, P., Lázár, V., … Pál, C. (2016). A highly precise and portable genome engineering method allows comparison of mutational effects across bacterial species. *Proceedings of the National Academy of Sciences of the United States of America*, *113*, 2502–2507.

Oberhardt, M. A., Palsson, B. Ø., & Papin, J. A. (2009). Applications of genome-scale metabolic reconstructions. *Molecular Systems Biology*, *5*, 1–15.

Ohno, S., Furusawa, C., & Shimizu, H. (2013). In silico screening of triple reaction knockout *Escherichia coli* strains for overproduction of useful metabolites. *Journal of Bioscience and Bioengineering*, *115*, 221–228.

Ohno, S., Shimizu, H., & Furusawa, C. (2014). FastPros: Screening of reaction knockout strategies for metabolic engineering. *Bioinformatics*, *30*, 981–987.

Orth, J. D., Thiele, I., & Palsson, B. Ø. (2010). What is flux balance analysis? *Nature Biotechnology*, *28*, 245–248.

Ow, D. S. W., Lee, D. Y., Yap, M. G. S., & Oh, S. K. W. (2009). Identification of cellular objective for elucidating the physiological state of plasmid-bearing *Escherichia coli* using genome-scale in Silico analysis. *Biotechnology Progress*, *25*, 61–67.

Sandberg, T. E., Pedersen, M., LaCroix, R., Ebrahim, A., Bonde, M., Herrgard, M. J., … Feist, A. M. (2014). Evolution of *escherichia coli* to 42 °C and subsequent genetic engineering reveals adaptive mechanisms and novel mutations. *Molecular Biology and Evolution*, *31*, 2647–2662.

Schellenberger, J., Que, R., Fleming, R. M. T., Thiele, I., Orth, J. D., Feist, A. M., … Palsson, B. Ø. (2011). Quantitative prediction of cellular metabolism with constraint-based models: The COBRA Toolbox v2.0. *Nature Protocols*, *6*, 1290–1307.

Schuetz, R., Kuepfer, L., & Sauer, U. (2007). Systematic evaluation of objective functions for predicting intracellular fluxes in *Escherichia coli*. *Molecular Systems Biology*, *3*, 1–15.

Takeya, M., Hirai, M. Y., & Osanai, T. (2017). Allosteric inhibition of phosphoenolpyruvate carboxylases is determined by a single amino acid residue in cyanobacteria. *Scientific reports*, *7*, 41080–41088.

Thomason, L. C., Costantino, N., & Court, D. L. (2007). *E. coli* genome manipulation by P1 transduction. *Current Protocols in Molecular Biology*, Chapter 1:Unit 1.17, 1:17.

Tokuyama, K., Ohno, S., Yoshikawa, K., Hirasawa, T., Tanaka, S., Furusawa, C., & Shimizu, H. (2014). Increased 3-hydroxypropionic acid production from glycerol, by modification of central metabolism in *Escherichia coli*. *Microbial Cell Factories*, *13*, 64.

Varma, A., & Palsson B. Ø. (1994). Stoichiometric flux balance models quantitatively predict growth and metabolic by-product secretion in wild-type *Escherichia coli* W3110. *Applied and Environmental Microbiology*, *60*(10), 3724–3731.

Xu, P., Ranganathan, S., Fowler, Z. L., Maranas, C. D., & Koffas, M. A. G. (2011). Genome-scale metabolic network modeling results in minimal interventions that cooperatively force carbon flux towards malonyl-CoA. *Metabolic Engineering*, *13*, 578–587.

Yim, H., Haselbeck, R., Niu, W., Pujol-Baxley, C., Burgard, A., Boldt, J., … Van Dien, S. (2011). Metabolic engineering of *Escherichia coli* for direct production of 1,4-butanediol. *Nature Chemical Biology*, *7*, 445–452.

Zhi, S., Banting, G. S., Ruecker, N. J., & Neumann, N. F. (2017). Stress resistance in naturalised waste water *E. coli* strains. *Journal of Environmental Engineering and Science*, *12*, 42–50.

SUPPORTING INFORMATION

Additional Supporting Information may be found online in the supporting information tab for this article.

How to cite this article: Tokuyama K, Toya Y, Horinouchi T, Furusawa C, Matsuda F, Shimizu H. Application of adaptive laboratory evolution to overcome a flux limitation in an *Escherichia coli* production strain. *Biotechnology and Bioengineering*. 2018;115:1542–1551. https://doi.org/10.1002/bit.26568